

# Synthesis, Stability, and Complexation Behavior of Isolable Salen-Type $N_2S_2$ and $N_2SO$ Ligands Based on Thiol and Oxime Functionalities<sup>†</sup>

Shigehisa Akine, Ayako Akimoto, Takuya Shiga,<sup>‡</sup> Hiroki Oshio,<sup>‡</sup> and Tatsuya Nabeshima\*

Graduate School of Pure and Applied Sciences, University of Tsukuba, Tsukuba, Ibaraki 305-8571, Japan

Received July 31, 2007

The new salen-type  $N_2S_2$  tetradentate ligands,  $H_2L^1$  and  $H_2L^2$ , which have a donor set comprising oxime and thiol groups, were synthesized. These ligands are obtained as isolable colorless crystals, whereas the imine analogues are too unstable to be isolated. The unsymmetrical  $N_2SO$  ligands,  $H_2L^3$  and  $H_2L^4$ , were also obtained as stable compounds. When ligands  $H_2L^1$ – $H_2L^4$  are heated above the melting points, they mainly decompose via cleavage of the N–O bonds of a thiosalicylaldoxime moiety to give 1,2-benzisothiazole derivatives. The complexation of the  $N_2S_2$  ligands ( $H_2L^1$  and  $H_2L^2$ ) with nickel(II) acetate afforded square-planar mononuclear complexes  $[Ni(L^1)]$  and  $[Ni(L^2)]$ , respectively. In contrast, the complexation of the  $N_2SO$  ligand  $H_2L^3$  with nickel(II) acetate resulted in cleavage of the N–O bond, giving a tetranuclear complex having a cubane-type  $Ni_4O_4$  core. The N–O bonds of  $H_2L^1$ – $H_2L^4$  are more readily cleaved when the ligands are allowed to react with copper(II) acetate. In these cases, the alkoxo-bridged dinuclear complexes having a Cu–O–Cu–O four-membered ring are obtained. On the other hand, mononuclear complexes can be obtained by complexation of the ligands ( $H_2L^1$  or  $H_2L^3$ ) with palladium(II) acetate without N–O bond cleavage.

## Introduction

Salen is a chelate ligand consisting of two nitrogen and two oxygen donors, capable of forming stable metal complexes.<sup>1</sup> Various functional salen–metal complexes have been synthesized by complexation with the appropriate metal sources. It is important to introduce suitable functional groups into the organic moiety of metal complexes in order to improve or tune the properties of these metal complexes.<sup>2,3</sup> The introduction of bulky and chiral groups is crucial for the highly enantioselective manganese–salen catalysts,<sup>2</sup> and electron-donating and -withdrawing groups are utilized to finely tune the nonlinear optical properties of the copper(II) complexes of the salen analogues.<sup>3</sup> Such functional groups are mainly introduced into the benzene rings of salicylaldi-

mine or into the  $CH_2CH_2$  bridge. There are also some reports on modification of the methylene chain length of the salen complexes, including longer salen analogues (trialkylene, tetraalkylene, or longer alkylene chains).<sup>4</sup> The chain length of the salen complexes is one of the important factors that affects the electrochemical and spectroscopic properties of the metal center.

If a heteroatom is directly connected to the  $sp^2$  nitrogen donors, the properties of the  $N_2O_2$  coordination site drastically change (Chart 1). There are some examples of the salen-type ligand containing  $C=N-N$  nitrogen donors instead of the  $C=N-C$  imine moiety.<sup>5</sup> Recently, we reported the oxime-type salen ligand “salamo”, which is an analogue of salen; i.e., the imine  $C=N-C$  moieties of salen are replaced by  $C=N-O$  oxime bonds.<sup>6</sup> The salamo ligands exhibited a

<sup>†</sup> Dedicated to Professor Renji Okazaki on the occasion of his 70th birthday.

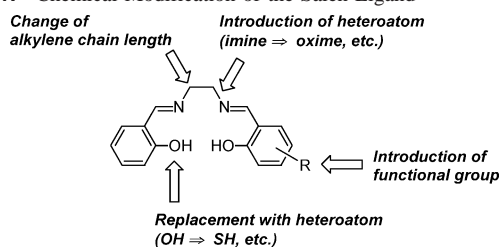
\* To whom correspondence should be addressed. E-mail: nabesima@chem.tsukuba.ac.jp.

<sup>‡</sup> Responsible for the magnetic measurements.

- (1) (a) Pfeiffer, P.; Breith, E.; Lübke, E.; Tsumaki, T. *Liebigs Ann. Chem.* **1933**, 503, 84–130. (b) Pfeiffer, P.; Hesse, T.; Pfitzner, H.; Scholl, W.; Thielert, H. *J. Prakt. Chem.* **1937**, 149, 217–296.
- (2) (a) Jacobsen, E. N. In *Catalytic Asymmetric Synthesis*; Ojima, I., Ed.; VCH: New York, 1993. (b) Katsuki, T. *Coord. Chem. Rev.* **1995**, 140, 189–214.
- (3) Rigamonti, L.; Demartin, F.; Forni, A.; Righetto, S.; Pasini, A. *Inorg. Chem.* **2006**, 45, 10976–10989.

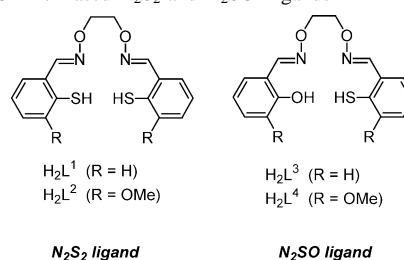
- (4) (a) Mockler, G. M.; Chaffey, G. W.; Sinn, E.; Wong, H. *Inorg. Chem.* **1972**, 11, 1308–1314. (b) Chjo, K.-H.; Jeong, B.-G.; Kim, J.-H.; Jeon, S.; Rim, C.-P.; Choi, Y.-K. *Bull. Korean Chem. Soc.* **1997**, 18, 850–856. (c) Kasumov, V. T.; Köksal, F. *Spectrochim. Acta* **2005**, A61, 225–231.
- (5) (a) Narang, K. K.; Lal, R. A. *Curr. Sci.* **1977**, 46, 401–403. (b) Yampol'skaya, M. A.; Shova, S. G.; Gerbeleu, N. V.; Simonov, Y. A.; Bel'skii, V. K.; Dvorkin, A. A. *Russ. J. Inorg. Chem.* **1983**, 28, 984–989. (c) Palanchuk, S. V.; Lipkovskii, Y.; Arion, V. B.; Simonov, Y. A.; Gerbeleu, N. V. *Russ. J. Coord. Chem.* **1995**, 21, 884–887. (d) Ardakani, M. M.; Sadeghi, A.; Salavati-Niasari, M. *Talanta* **2005**, 66, 837–843.

Chart 1. Chemical Modification of the Salen Ligand



very high stability that resisted recombination of the C=N bonds compared to the parent salen and are useful for the construction of helical metalloarchitectures.<sup>6a,7,8</sup>

To change the coordination environment of the salen-type  $N_2O_2$  ligand, the phenolic oxygen can be replaced by other elements, e.g., sulfur. The  $N_2S_2$  ligand tsalen and its analogues can form metal complexes with a variety of metal sources because of the high coordination ability of the soft sulfur donors.<sup>9–15</sup> The uncomplexed tsalen ligand, however, is known as an unstable compound<sup>9</sup> that readily undergoes cyclization to give bicyclic dithiocin derivatives.<sup>9,16</sup> Such an instability is attributed to the high reactivity of thiols with aldimine groups. Consequently, some of the tsalen–metal complexes have been synthesized without isolation of the

Chart 2. Oxime-Based  $N_2S_2$  and  $N_2SO$  Ligands

free ligand using a one-pot procedure.<sup>10</sup> Alternatively, they are prepared via easily accessible synthetic intermediates, the reaction of bis(thiosalicylaldehyde)metal complexes with diamines,<sup>9,11</sup> transmetalation of  $[Ti_2(\text{tsalen})]$ ,<sup>12</sup> metalation of *tert*-butyl-protected tsalen ligand,<sup>13</sup> or the reaction of 2,2'-dithiodibenzaldehyde with ethylenediaminatometal complexes,<sup>14</sup> etc. However, it is important to develop an isolable  $N_2S_2$ -type salen ligand especially when they are utilized as a building block of higher-order metalloarchitectures. Furthermore, metal complexes of the  $N_2S_2$  chelate ligand other than tsalen have recently attracted much attention because they are used as a model for the nickel reaction centers of enzymes, such as bifunctional carbon monoxide dehydrogenase/acetyl-CoA synthase and nickel-containing superoxide dismutase.<sup>17</sup> Such  $N_2S_2$  ligands containing thiolato groups are also useful as a building block for heterometallic clusters.<sup>18</sup>

In contrast, thiosalicylaldoximes are more stable than thiosalicylaldimines. Some thiosalicylaldoxime derivatives can form a mononuclear square-planar nickel(II) complex.<sup>19</sup> We expect that the oxime functionality is suitable for the  $sp^2$  nitrogen donor for the isolable tsalen-type  $N_2S_2$  ligand. We now describe the synthesis of oxime-based salen-type  $N_2S_2$  ligands,  $H_2L^1$  and  $H_2L^2$  (Chart 2), i.e., 1,2-bis(thiosalicylideneaminoxime)ethane (tsalamo), which are much more stable than their imine analogue, tsalen.<sup>20</sup> In addition, unsymmetrical ligands,  $H_2L^3$  and  $H_2L^4$ , having an  $N_2SO$  donor set were also prepared. We investigated the influence of the oxime groups on the stability and complexation behavior using spectroscopic and crystallographic methods.

## Experimental Section

**General Procedures.** All experiments were carried out in air unless otherwise noted. Commercial dichloromethane, methanol, acetonitrile, and hexane were used without further purification. Silica gel chromatography was performed by Kanto Silica Gel 60N (spherical, neutral). Gel permeation chromatography (GPC) was

- (6) (a) Akine, S.; Taniguchi, T.; Nabeshima, T. *Chem. Lett.* **2001**, 682–683. (b) Akine, S.; Taniguchi, T.; Dong, W.; Masubuchi, S.; Nabeshima, T. *J. Org. Chem.* **2005**, *70*, 1704–1711.
- (7) (a) Akine, S.; Taniguchi, T.; Nabeshima, T. *Angew. Chem., Int. Ed.* **2002**, *41*, 4670–4673. (b) Akine, S.; Taniguchi, T.; Saiki, T.; Nabeshima, T. *J. Am. Chem. Soc.* **2005**, *127*, 540–541. (c) Akine, S.; Matsumoto, T.; Taniguchi, T.; Nabeshima, T. *Inorg. Chem.* **2005**, *44*, 3270–3274. (d) Akine, S.; Taniguchi, T.; Nabeshima, T. *Tetrahedron Lett.* **2006**, *47*, 8419–8422. (e) Akine, S.; Taniguchi, T.; Nabeshima, T. *J. Am. Chem. Soc.* **2006**, *128*, 15765–15774. (f) Akine, S.; Taniguchi, T.; Matsumoto, T.; Nabeshima, T. *Chem. Commun.* **2006**, 4961–4963. (g) Akine, S.; Kagiya, S.; Nabeshima, T. *Inorg. Chem.* **2007**, *46*, 9525–9527.
- (8) For related salamo–metal complexes, see: (a) Akine, S.; Taniguchi, T.; Nabeshima, T. *Inorg. Chem.* **2004**, *43*, 6142–6144. (b) Akine, S.; Taniguchi, T.; Nabeshima, T. *Chem. Lett.* **2006**, *35*, 604–605. (c) Akine, S.; Dong, W.; Nabeshima, T. *Inorg. Chem.* **2006**, *45*, 4677–4684. (d) Akine, S.; Sunaga, S.; Taniguchi, T.; Miyazaki, H.; Nabeshima, T. *Inorg. Chem.* **2007**, *46*, 2959–2961.
- (9) (a) Corrigan, M. F.; West, B. O. *Aust. J. Chem.* **1976**, *29*, 1413–1427. (b) Marini, P. J.; Murray, K. S.; West, B. O. *J. Chem. Soc., Dalton Trans.* **1983**, 143–151.
- (10) (a) Hoyer, E.; Lorenz, B. Z. *Chem.* **1968**, *8*, 28–29. (b) Bertini, I.; Sacconi, L.; Speroni, G. P. *Inorg. Chem.* **1972**, *11*, 1323–1326. (c) Engeseth, H. R.; McMillin, D. R.; Ulrich, E. L. *Inorg. Chim. Acta* **1982**, *67*, 145–149. (d) Dutton, J. C.; Fallon, G. D.; Murray, K. S. *Inorg. Chem.* **1988**, *27*, 34–38.
- (11) (a) Marini, P. J.; Murray, K. S.; West, B. O. *J. Chem. Soc., Chem. Commun.* **1981**, 726–728. (b) Marini, P. J.; Berry, K. J.; Murray, K. S.; West, B. O.; Irving, M.; Clark, P. E. *J. Chem. Soc., Dalton Trans.* **1983**, 879–884.
- (12) Fallon, G. D.; Gatehouse, B. M.; Marini, P. J.; Murray, K. S.; West, B. O. *J. Chem. Soc., Dalton Trans.* **1984**, 2733–2739.
- (13) (a) Yamamura, T.; Tadokoro, M.; Kuroda, R. *Chem. Lett.* **1989**, 1245–1246. (b) Yamamura, T.; Tadokoro, M.; Tanaka, K.; Kuroda, R. *Bull. Chem. Soc. Jpn.* **1993**, *66*, 1984–1990. (c) Henderson, R. K.; Bouwman, E.; Reedijk, J.; Powell, A. K. *Acta Crystallogr.* **1996**, *C52*, 2696–2698. (d) Smeets, W. J. J.; Spek, A. L.; Henderson, R. K.; Bouwman, E.; Reedijk, J. *Acta Crystallogr.* **1997**, *C53*, 1564–1566.
- (14) (a) Goswami, N.; Eichhorn, D. M. *Inorg. Chem.* **1999**, *38*, 4329–4333. (b) Goswami, N.; Eichhorn, D. M. *Inorg. Chim. Acta* **2000**, *303*, 271–276.
- (15) (a) Fallon, G. D.; Gatehouse, B. M. *Acta Crystallogr.* **1976**, *B32*, 97–101. (b) Gomes, L.; Pereira, E.; de Castro, B. *Acta Crystallogr.* **1999**, *C55*, 1061–1063.
- (16) (a) Corrigan, M. F.; Rae, I. D.; West, B. O. *Aust. J. Chem.* **1978**, *31*, 587–594. (b) Toste, F. D.; Lough, A. J.; Still, I. W. *J. Tetrahedron Lett.* **1995**, *36*, 6619–6622.

- (17) (a) *The Bioinorganic Chemistry of Nickel*; Lancaster, J. R., Jr., Ed.; VCH Publishers: New York, 1988. (b) Halcrow, M. A.; Christou, G. *Chem. Rev.* **1994**, *94*, 2421–2481. (c) Doukov, T. I.; Iverson, T. M.; Seravalli, J.; Ragsdale, S. W.; Drennan, C. L. *Science* **2002**, *298*, 567–572. (d) Wuerges, J.; Lee, J.-W.; Yim, Y.-I.; Yim, H.-S.; Kang, S.-O.; Carugo, K. D. *Proc. Natl. Acad. Sci. U.S.A.* **2004**, *101*, 8569–8574.
- (18) Golden, M. L.; Rampersad, M. V.; Reibenspies, J. H.; Darensbourg, M. Y. *Chem. Commun.* **2003**, 1824–1825.
- (19) (a) Nagata, K. *Chem. Pharm. Bull.* **1969**, *17*, 661–668. (b) Vasil'chenko, I. S.; Mistryukov, A. E.; Kochin, S. G.; Sergienko, V. S.; Porai-Koshits, M. A.; Garnovskii, A. D. *Russ. J. Inorg. Chem.* **1992**, *37*, 527–529.
- (20) For the preliminary report on  $H_2L^1$  and  $[Ni(L^1)]$ , see: Akine, S.; Nabeshima, T. *Inorg. Chem.* **2005**, *44*, 1205–1207.

performed on an LC908 (Japan Analytical Industry Co., Ltd.) equipped with JAIGEL 1H and 2H columns using chloroform as the eluent. Melting points were determined on a Yanaco melting point apparatus and are not corrected.  $^1H$  and  $^{13}C$  NMR spectra were recorded on a Bruker ARX400 (400 and 100 MHz) spectrometer. Mass spectra were recorded on an Applied Biosystems QStar Pulsar *i* spectrometer (electrospray ionization time of flight, ESI-TOF, positive mode) or a Shimadzu QP-5000 spectrometer (electron impact, EI, 70 eV, GC-MS). UV-vis absorption spectra were recorded on a UBest V560 spectrophotometer using a 10-mm-path-length quartz cell.

**Materials.** 1,2-Bis(aminoxy)ethane,<sup>21</sup> thiosalicylaldehyde (**1**),<sup>16b</sup> salicylaldehyde *O*-[2-(aminoxy)ethyl]oxime (**5**),<sup>6b</sup> and 2-hydroxy-3-methoxybenzaldehyde *O*-[2-(aminoxy)ethyl]oxime (**6**)<sup>6b</sup> (see Scheme 1 for structures) were prepared according to the reported procedures. 2-Mercapto-3-methoxybenzaldehyde (**2**)<sup>22</sup> was synthesized from 2-methoxybenzenethiol by a procedure analogous to that for **1**.<sup>16b</sup>

**Synthesis of the  $N_2S_2$  Ligand  $H_2L^1$ .** A solution of 1,2-bis(aminoxy)ethane (72.6 mg, 0.79 mmol) in dichloromethane (5 mL) was added to a solution of **1** (1.6 mmol) in dichloromethane, and the resulting solution was kept at room temperature for 5 h. The mixture was directly subjected to column chromatography on silica gel and eluted with dichloromethane to give ligand  $H_2L^1$  as colorless crystals (123 mg, 47%): mp 61–62 °C;  $^1H$  NMR (400 MHz,  $CDCl_3$ )  $\delta$  4.53 (s, 4H), 4.61 (s, 2H), 7.16 (td,  $J = 7.4$  and 1.5 Hz, 2H), 7.20 (td,  $J = 7.4$  and 1.5 Hz, 2H), 7.32 (dd,  $J = 7.4$  and 1.5 Hz, 2H), 7.52 (dd,  $J = 7.4$  and 1.5 Hz, 2H), 8.42 (s, 2H);  $^{13}C$  NMR (100 MHz,  $CDCl_3$ )  $\delta$  72.8 ( $CH_2$ ), 125.6 (CH), 129.4 (C), 129.5 (CH), 129.9 (CH), 131.4 (CH), 132.1 (C), 149.2 (CH). Anal. Calcd for  $C_{16}H_{16}N_2O_2S_2$ : C, 57.81; H, 4.85; N, 8.43. Found: C, 57.67; H, 4.74; N, 7.72.

**Synthesis of the  $N_2S_2$  Ligand  $H_2L^2$ .** A solution of 1,2-bis(aminoxy)ethane (180 mg, 1.95 mmol) and **2** (629 mg, 3.74 mmol) in dichloromethane (20 mL) was stirred at room temperature for 1.5 h. After removal of the solvent, the crude  $H_2L^2$  was purified by GPC, followed by column chromatography on silica gel (dichloromethane) to give  $H_2L^2$  (314 mg, 43%) as pale-yellow crystals: mp 82–85 °C;  $^1H$  NMR (400 MHz,  $CDCl_3$ )  $\delta$  3.92 (s, 6H), 4.53 (s, 4H), 4.95 (s, 2H), 6.86 (dd,  $J = 7.9$  and 1.0 Hz, 2H), 7.11 (t,  $J = 7.9$  Hz, 2H), 7.23 (dd,  $J = 7.9$  and 1.0 Hz, 2H), 8.44 (s, 2H);  $^{13}C$  NMR (100 MHz,  $CDCl_3$ )  $\delta$  56.2 ( $CH_3$ ), 72.7 ( $CH_2$ ), 111.0 (CH), 121.4 (CH), 122.2 (C), 125.1 (CH), 129.8 (C), 148.6 (CH), 154.6 (C). Anal. Calcd for  $C_{18}H_{20}N_2O_4S_2$ : C, 55.08; H, 5.14; N, 7.14. Found: C, 54.80; H, 5.04; N, 6.86.

**Synthesis of the  $N_2SO$  Ligand  $H_2L^3$ .** A solution of **1** (0.73 mmol) in dichloromethane (2 mL) was added to a solution of oxime **5** (140 mg, 0.71 mmol) in dichloromethane (8 mL) and the resulting solution was stirred for 4 h at room temperature. After the removal of the solvent, the residue was subjected to column chromatography on silica gel (dichloromethane/hexane, 1:1) to afford ligand  $H_2L^3$  (109 mg, 48%) as colorless crystals, mp 51–52 °C,  $^1H$  NMR (400 MHz,  $CDCl_3$ )  $\delta$  4.50 (s, 4H), 4.53 (s, 1H), 6.89 (t,  $J = 7.4$  Hz, 1H), 6.97 (d,  $J = 8.4$  Hz, 1H), 7.13–7.21 (m, 3H), 7.27 (td,  $J = 7.4$ , 1.4 Hz, 1H), 7.31 (dd,  $J = 7.4$ , 1.4 Hz, 1H), 7.51 (dd,  $J = 7.4$  and 1.4 Hz, 1H), 8.23 (s, 1H), 8.42 (s, 1H), 9.82 (s, 1H);  $^{13}C$  NMR (100 MHz,  $CDCl_3$ )  $\delta$  72.7 ( $CH_2$ ), 73.0 ( $CH_2$ ), 116.2 (C), 116.7 (CH), 119.6 (CH), 125.6 (CH), 129.3 (C), 129.6 (CH), 129.8 (CH), 130.8 (CH), 131.26 (CH), 131.35 (CH), 132.0 (C), 149.4 (CH),

152.1 (CH), 157.4 (C). Anal. Calcd for  $C_{16}H_{16}N_2O_3S$ : C, 60.74; H, 5.10; N, 8.85. Found: C, 60.72; H, 5.12; N, 8.34.

**Synthesis of the  $N_2SO$  Ligand  $H_2L^4$ .** A solution of **2** (84.5 mg, 0.50 mmol) in dichloromethane (4 mL) was added to oxime **6** (91.6 mg, 0.40 mmol), and the resulting solution was stirred for 4.5 h at room temperature. After removal of the solvent, the residue was subjected to column chromatography on silica gel (dichloromethane/hexane, 1:1, and then dichloromethane) to afford  $H_2L^4$  (84.2 mg, 55%) as colorless crystals: mp 85–86 °C;  $^1H$  NMR (400 MHz,  $CDCl_3$ )  $\delta$  3.90 (s, 6H), 4.50 (s, 4H), 4.90 (br s, 1H), 6.81 (dd,  $J = 7.6$  and 1.8 Hz, 1H), 6.85 (t,  $J = 7.6$  Hz, 1H), 6.85 (d,  $J = 7.7$  Hz, 1H), 6.90 (dd,  $J = 7.6$  and 1.8 Hz, 1H), 7.09 (t,  $J = 7.7$  Hz, 1H), 7.22 (d,  $J = 7.7$  Hz, 1H), 8.25 (s, 1H), 8.43 (s, 1H), 9.82 (s, 1H);  $^{13}C$  NMR (100 MHz,  $CDCl_3$ )  $\delta$  56.18 ( $CH_3$ ), 56.23 ( $CH_3$ ), 72.4 ( $CH_2$ ), 73.1 ( $CH_2$ ), 111.1 (CH), 113.5 (CH), 116.5 (C), 119.4 (CH), 121.4 (CH), 122.3 (C), 122.4 (CH), 125.1 (CH), 129.8 (C), 147.1 (C), 148.2 (C), 148.8 (CH), 151.9 (CH), 154.7 (C). Anal. Calcd for  $C_{18}H_{20}N_2O_3S \cdot 0.25H_2O$ : C, 56.75; H, 5.42; N, 7.35. Found: C, 56.78; H, 5.28; N, 7.19.

**General Procedure for Thermolysis of Ligands  $H_2L^1$ – $H_2L^4$ .** A sample of ligands  $H_2L^1$ – $H_2L^4$  was placed in a flask under an argon atmosphere and was heated at 150 °C for 1–2 h. The reaction mixture was separated by GPC or silica gel chromatography.

**Thermolysis of  $H_2L^1$ .** From  $H_2L^1$  (40.0 mg, 0.12 mmol), 1,2-benzisothiazole (**7**; 17.0 mg, 53%) was obtained. **7**:  $^1H$  NMR (400 MHz,  $CDCl_3$ )  $\delta$  7.44 (t,  $J = 7.7$  Hz, 1H), 7.53 (t,  $J = 7.7$  Hz, 1H), 7.97 (d,  $J = 7.7$  Hz, 1H), 8.07 (d,  $J = 7.7$  Hz, 1H), 8.92 (s, 1H);  $^{13}C$  NMR (100 MHz,  $CDCl_3$ )  $\delta$  119.6 (CH), 124.0 (CH), 124.9 (CH), 127.8 (CH), 136.0 (C), 151.7 (C), 154.9 (CH); GC-MS  $m/z$  135 ( $M^+$ ). The spectra were consistent with those reported in the literature.<sup>23</sup>

**Thermolysis of  $H_2L^2$ .** From  $H_2L^2$  (8.8 mg, 0.022 mmol), 7-methoxy-1,2-benzisothiazole (**8**; 7.4 mg, 100%) was obtained. **8**:  $^1H$  NMR (400 MHz,  $CDCl_3$ )  $\delta$  4.01 (s, 3H), 6.88 (d,  $J = 7.9$  Hz, 1H), 7.39 (t,  $J = 7.9$  Hz, 1H), 7.64 (d,  $J = 7.9$  Hz, 1H), 8.87 (s, 1H);  $^{13}C$  NMR (100 MHz,  $CDCl_3$ )  $\delta$  55.8 ( $CH_3$ ), 106.6 (CH), 116.0 (CH), 126.8 (CH), 137.9 (C), 141.9 (C), 152.9 (C), 154.9 (CH); GC-MS  $m/z$  165 ( $M^+$ ). The spectra were consistent with those reported in the literature.<sup>22</sup>

**Thermolysis of  $H_2L^3$ .** From  $H_2L^3$  (40.7 mg, 0.13 mmol), **7** (9.8 mg, 56%) and salicylaldehyde *O*-(2-hydroxyethyl)oxime (**9**; 17.2 mg, 74%) were obtained. **9**: pale-yellow oil;  $^1H$  NMR (400 MHz,  $CDCl_3$ )  $\delta$  1.83 (br s, 1H), 3.94 (br t, 2H), 4.31 (t,  $J = 4.5$  Hz, 2H), 6.92 (td,  $J = 7.5$  and 1.1 Hz, 1H), 6.99 (d,  $J = 8.1$  Hz, 1H), 7.17 (dd,  $J = 7.5$  and 1.8 Hz, 1H), 7.30 (ddd,  $J = 8.1$ , 7.5, and 1.8 Hz, 1H), 8.24 (s, 1H), 9.72 (s, 1H);  $^{13}C$  NMR (100 MHz,  $CDCl_3$ )  $\delta$  61.1 ( $CH_2$ ), 75.9 ( $CH_2$ ), 116.1 (C), 116.8 (CH), 119.7 (CH), 130.9 (CH), 131.5 (CH), 152.3 (CH), 157.4 (C); GC-MS  $m/z$  181 ( $M^+$ ). Anal. Calcd for  $C_9H_{11}NO_3$ : C, 59.66; H, 6.12; N, 7.73. Found: C, 59.75; H, 6.11; N, 7.42.

**Thermolysis of  $H_2L^4$ .** From  $H_2L^4$  (22.6 mg, 0.060 mmol), **8** (4.5 mg, 45%) and 2-hydroxy-3-methoxybenzaldehyde *O*-(2-hydroxyethyl)oxime (**10**, 9.5 mg, 75%) were obtained. **10**: pale-yellow crystals; mp 87–88 °C;  $^1H$  NMR (400 MHz,  $CDCl_3$ )  $\delta$  1.97 (s, 1H), 3.91 (s, 3H), 3.93 (t,  $J = 4.4$  Hz, 2H), 4.31 (t,  $J = 4.4$  Hz, 2H), 6.83 (dd,  $J = 7.7$  and 2.0 Hz, 1H), 6.87 (t,  $J = 7.7$  Hz, 1H), 6.92 (dd,  $J = 7.7$  and 2.0 Hz, 1H), 8.24 (s, 1H), 9.61 (s, 1H);  $^{13}C$  NMR (100 MHz,  $CDCl_3$ )  $\delta$  56.2 ( $CH_3$ ), 61.2 ( $CH_2$ ), 75.9 ( $CH_2$ ), 113.5 (CH), 116.4 (C), 119.5 (CH), 122.2 (CH), 146.9 (C), 148.0

(21) Dixon, D. W.; Weiss, R. H. *J. Org. Chem.* **1984**, *49*, 4487–4494.

(22) Rahman, L. K. A.; Scrowston, R. M. *J. Chem. Soc., Perkin Trans. 1* **1983**, 2973–2977.

(23) (a) Rynbrandt, R. H.; Balgoyen, D. P. *J. Org. Chem.* **1978**, *43*, 1824–1825. (b) Creed, T.; Leardini, R.; McNab, H.; Nanni, D.; Nicolson, I. S.; Reed, D. *J. Chem. Soc., Perkin Trans. 1* **2001**, 1079–1085.



(C), 151.7 (CH); GC-MS  $m/z$  211 ( $M^+$ ). Anal. Calcd for  $C_{10}H_{13}NO_4$ : C, 56.86; H, 6.20; N, 6.63. Found: C, 56.74; H, 6.25; N, 6.44.

**Synthesis of  $[Ni(L^1)]$ .** A solution of nickel(II) acetate tetrahydrate (50 mg, 0.20 mmol) in methanol (1 mL) was added to a solution of  $H_2L^1$  (66 mg, 0.20 mmol) in dichloromethane (1 mL). After the solvent was removed, the residue was recrystallized from dichloromethane/methanol to afford  $[Ni(L^1)]$  (53.4 mg, 67%) as dark-brown crystals:  $^1H$  NMR (400 MHz,  $CDCl_3$ )  $\delta$  4.85 (s, 4H), 7.06 (td,  $J = 7.8$  and 1.2 Hz, 2H), 7.17 (td,  $J = 7.8$  and 1.2 Hz, 2H), 7.22 (dd,  $J = 7.8$  and 1.2 Hz, 2H), 7.72 (d,  $J = 7.8$  Hz, 2H), 8.16 (s, 2H); ESI-MS  $m/z$  388.0 for  $[Ni(L^1)]^+$ . Anal. Calcd for  $C_{16}H_{14}N_2NiO_2S_2$ : C, 49.39; H, 3.63; N, 7.20. Found: C, 49.83; H, 3.94; N, 6.98.

**Synthesis of  $[Ni(L^2)]$ .** A solution of nickel(II) acetate tetrahydrate (6.6 mg, 0.027 mmol) in methanol (4 mL) was mixed with a solution of  $H_2L^2$  (10.0 mg, 0.026 mmol) in dichloromethane (4 mL). After the addition of hexane, the precipitates were collected to afford  $[Ni(L^2)]$  (7.5 mg, 65%) as brown crystals. Single crystals suitable for X-ray crystallographic analysis were obtained by recrystallization from acetonitrile.  $[Ni(L^2)]$ :  $^1H$  NMR (400 MHz,  $CD_3CN$ )  $\delta$  3.87 (s, 6H), 4.78 (s, 4H), 6.90 (dd,  $J = 7.7$  and 1.6 Hz, 2H), 7.05 (dd,  $J = 7.7$  and 1.6 Hz, 2H), 7.10 (t,  $J = 7.7$  Hz, 2H), 8.35 (s, 2H); ESI-MS  $m/z$  449.1 for  $[Ni(L^2) + H]^+$ . Anal. Calcd for  $C_{18}H_{18}N_2NiO_4S_2$ : C, 48.13; H, 4.04; N, 6.24. Found: C, 48.23; H, 4.13; N, 6.18.

**Reaction of  $H_2L^3$  with Nickel(II) Acetate.** A solution of  $H_2L^3$  (17.9 mg, 0.057 mmol) in dichloromethane (5 mL) was added to a solution of nickel(II) acetate tetrahydrate (14.1 mg, 0.057 mmol) in methanol (5 mL). The solution was concentrated to ca. 0.2 mL under reduced pressure, and acetonitrile (ca. 0.8 mL) was added to the solution. Bluish-green crystals were collected to give tetranuclear complex  $[Ni_4(L^5)_2(HL^5)_2(OAc)_2]$  (7.8 mg, 51%). Anal. Calcd for  $C_{40}H_{44}N_4Ni_4O_{16} \cdot 0.5CH_3CN$ : C, 45.09; H, 4.20; N, 5.77. Found: C, 45.46; H, 4.34; N, 5.71.

**General Procedure for the Reaction of Ligands  $H_2L^1-H_2L^4$  with Copper(II) Acetate.** A solution of ligands ( $H_2L^1-H_2L^4$ ) in dichloromethane was added to a solution of an equimolar amount of copper(II) acetate monohydrate in methanol, and the resulting solution was kept at room temperature. Crystals formed in the solution were collected on a suction filter.

**Reaction of  $H_2L^1$  with Copper(II) Acetate.** From  $H_2L^1$  (133 mg, 0.40 mmol) and copper(II) acetate monohydrate (80 mg, 0.40 mmol),  $[Cu_2(L^7)_2]$  was obtained (yield 1.8 mg, 2%) as dark-brown crystals. Anal. Calcd for  $C_{18}H_{18}Cu_2N_2O_4S_2$ : C, 41.77; H, 3.51; N, 5.41. Found: C, 41.79; H, 3.38; N, 5.23.

**Reaction of  $H_2L^2$  with Copper(II) Acetate.** From  $H_2L^2$  (105 mg, 0.27 mmol) and copper(II) acetate monohydrate (53 mg, 0.27 mmol),  $[Cu_2(L^8)_2]$  was obtained (yield 6.5 mg, 8%) as dark-brown crystals. Anal. Calcd for  $C_{20}H_{22}Cu_2N_2O_6S_2 \cdot 0.5H_2O$ : C, 40.95; H, 3.95; N, 4.78. Found: C, 40.70; H, 4.09; N, 4.48.

**Reaction of  $H_2L^3$  with Copper(II) Acetate.** From  $H_2L^3$  (50 mg, 0.16 mmol) and copper(II) acetate monohydrate (32 mg, 0.16 mmol),  $[Cu_2(L^5)_2]$  was obtained (yield 19.9 mg, 52%) as dark-green crystals. Anal. Calcd for  $C_{18}H_{18}Cu_2N_2O_6 \cdot 0.5H_2O$ : C, 43.72; H, 3.87; N, 5.67. Found: C, 43.94; H, 3.73; N, 5.55.

**Reaction of  $H_2L^4$  with Copper(II) Acetate.** From  $H_2L^4$  (52 mg, 0.14 mmol) and copper(II) acetate monohydrate (28 mg, 0.14 mmol),  $[Cu_2(L^6)_2]$  were obtained (yield 19.7 mg, 52%) as dark-green crystals. Anal. Calcd for  $C_{20}H_{22}Cu_2N_2O_8 \cdot 0.5H_2O$ : C, 43.32; H, 4.18; N, 5.05. Found: C, 43.23; H, 4.01; N, 4.96.

**General Procedure for the Synthesis of Palladium(II) Complexes.** A solution of ligands ( $H_2L^1, H_2L^3$ ) in dichloromethane was

added to a solution of palladium(II) acetate (equimolar amount) in methanol. After the solution was concentrated, hexane was added to give a reddish-orange powder of the palladium(II) complex.

**Synthesis of  $[Pd(L^1)]$ .** From  $H_2L^1$  (17.7 mg, 0.053 mmol),  $[Pd(L^1)]$  (6.0 mg, 26%) was obtained:  $^1H$  NMR (400 MHz,  $CDCl_3$ )  $\delta$  4.74 (s, 4H), 7.04 (td,  $J = 7.7$  and 1.2 Hz, 2H), 7.21–7.25 (m, 4H), 7.75 (d,  $J = 7.7$  Hz, 2H), 8.27 (s, 2H); ESI-MS  $m/z$  437.0 for  $[Pd(L^1) + H]^+$ . Anal. Calcd for  $C_{16}H_{14}N_2O_2PdS_2 \cdot 0.5H_2O$ : C, 43.10; H, 3.39; N, 6.28. Found: C, 43.45; H, 3.34; N, 5.99.

**Synthesis of  $[Pd(L^3)]$ .** From  $H_2L^3$  (21.0 mg, 0.066 mmol),  $[Pd(L^3)]$  (13.2 mg, 47%) was obtained:  $^1H$  NMR (400 MHz,  $CDCl_3$ )  $\delta$  4.60 (t,  $J = 4.7$  Hz, 2H), 4.68 (t,  $J = 4.7$  Hz, 2H), 6.61 (t,  $J = 7.5$  Hz, 1H), 6.97 (d,  $J = 7.5$  Hz, 1H), 7.00 (t,  $J = 7.7$  Hz, 1H), 7.07 (dd,  $J = 7.7$  and 1.7 Hz, 1H), 7.21–7.31 (m, 3H), 7.75 (d,  $J = 7.7$  Hz, 1H), 8.04 (s, 1H), 8.18 (s, 1H); ESI-MS  $m/z$  421.0 for  $[Pd(L^3) + H]^+$ . Anal. Calcd for  $C_{16}H_{14}N_2O_3PdS$ : C, 45.67; H, 3.35; N, 6.66. Found: C, 45.78; H, 3.44; N, 6.31.

**X-ray Crystallographic Analysis.** Intensity data were collected on a Rigaku R-Axis Rapid diffractometer with Mo  $K\alpha$  radiation ( $\lambda = 0.71069 \text{ \AA}$ ). Reflection data were corrected for Lorentz and polarization factors and for absorption using the multiscan method. The structure was solved by Patterson methods (*DIRDIF 99*<sup>24</sup>) and refined by full-matrix least squares on  $F^2$  using *SHELXL 97*.<sup>25</sup> The crystallographic data are summarized in Table 1.

**Magnetic Measurements.** Magnetic data were obtained on powdered samples of  $[Ni_4(L^5)_2(HL^5)_2(OAc)_2] \cdot MeCN$  and  $[Cu_2(L^5)_2]$  with a Quantum Design model MPMS XL5 SQUID magnetometer. Magnetic susceptibility measurements were performed at 500 Oe in the 1.8–300 K temperature range, and diamagnetic corrections were applied by using Pascal's constants.<sup>26</sup>

## Results and Discussion

**Synthesis of the  $N_2S_2$  and  $N_2SO$  Ligands.** The synthesis of new  $N_2S_2$  ligands,  $H_2L^1$  and  $H_2L^2$ , is shown in Scheme 1. **1** and **2** were prepared by the ortho lithiation of the corresponding thiols followed by reaction with *N,N*-dimethylformamide.<sup>16b</sup> **1** was not isolated because this compound partly decomposes upon removal of the solvent.<sup>27</sup> For this reason, the compound was kept in solution and used for the next reaction without isolation. Compound **2** was obtained as a stable solid. The reaction of the thiosalicylaldehyde derivatives **1** and **2** with 1,2-bis(aminooxy)ethane<sup>21</sup> in dichloromethane afforded  $H_2L^1$  and  $H_2L^2$  in 47% and 43% yield, respectively. The  $N_2S_2$  ligands were isolable as colorless crystals with melting points of 61–62 °C ( $H_2L^1$ ) and 82–85 °C ( $H_2L^2$ ).

The stabilities of  $H_2L^1$  and  $H_2L^2$ , compared to those of the tsalen derivatives, are mainly due to the low reactivity of the C=N bonds toward nucleophiles. The inertness of the oxime C=N bonds is also useful for the synthesis of unsymmetrical ligands having an  $N_2SO$  donor set. When the ligands are based on the imine C=N bonds, the synthesis of

(24) Beurskens, P. T.; Beurskens, G.; de Gelder, R.; Garcia-Granda, S.; Gould, R. O.; Israel, R.; Smits, J. M. M. *The DIRDIF-99 program system*; Crystallography Laboratory, University of Nijmegen: Nijmegen, The Netherlands, 1999.

(25) Sheldrick, G. M. *SHELXL 97, Program for Crystal Structure Refinement*; University of Göttingen: Göttingen, Germany, 1997.

(26) Pascal, P. *Ann. Chim. Phys.* **1910**, *19*, 5–70.

(27) Gallagher, T.; Pardoe, D. A.; Porter, R. A. *Tetrahedron Lett.* **2000**, *41*, 5415–5418.

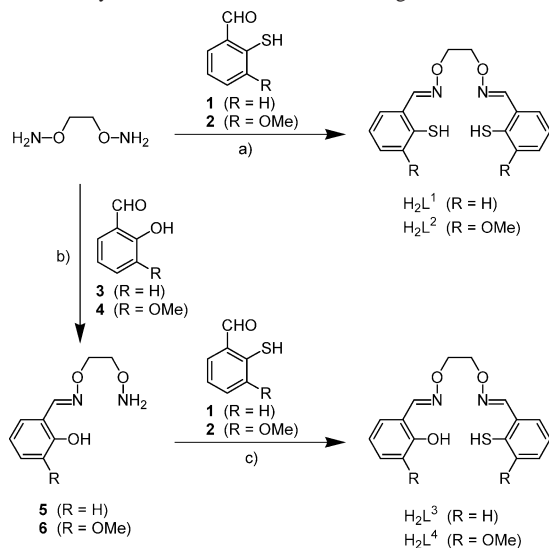
Table 1. Crystallographic Data

param	[Ni(L <sup>1</sup> )]	[Ni(L <sup>2</sup> )]	[Ni <sub>4</sub> (L <sup>5</sup> ) <sub>2</sub> (HL <sup>5</sup> ) <sub>2</sub> OAc) <sub>2</sub> ·MeCN	[Cu <sub>2</sub> (L <sup>7</sup> ) <sub>2</sub> ]
formula	C <sub>16</sub> H <sub>14</sub> N <sub>2</sub> NiO <sub>2</sub> S <sub>2</sub>	C <sub>18</sub> H <sub>18</sub> N <sub>2</sub> NiO <sub>4</sub> S <sub>2</sub>	C <sub>42</sub> H <sub>47</sub> N <sub>5</sub> Ni <sub>4</sub> O <sub>16</sub>	C <sub>18</sub> H <sub>18</sub> Cu <sub>2</sub> N <sub>2</sub> O <sub>4</sub> S <sub>2</sub>
cryst syst	monoclinic	orthorhombic	monoclinic	triclinic
space group	<i>P</i> 2 <sub>1</sub> / <i>a</i>	<i>Pca</i> 2 <sub>1</sub>	<i>P</i> 2 <sub>1</sub> / <i>n</i>	<i>P</i> $\bar{1}$
<i>a</i> /Å	8.0198(7)	8.243(3)	10.914(3)	5.737(4)
<i>b</i> /Å	19.6504(14)	15.427(6)	24.008(7)	8.386(7)
<i>c</i> /Å	9.8681(7)	14.466(5)	16.826(5)	10.552(6)
$\alpha$ /deg				84.74(3)
$\beta$ /deg	94.882(3)		90.773(12)	74.90(2)
$\gamma$ /deg				69.13(3)
<i>V</i> /Å <sup>3</sup>	1549.5(2)	1839.6(12)	4408(2)	458.0(6)
<i>Z</i>	4	4	4	1
<i>T</i> /K	150	120	120	120
<i>D</i> <sub>calc</sub> /g cm <sup>-3</sup>	1.668	1.622	1.677	1.877
R1 <sup>a</sup> [ <i>I</i> > 2 $\sigma$ ( <i>I</i> )]	0.0443	0.0202	0.0532	0.0228
wR2 <sup>a</sup> (all data)	0.1136	0.0481	0.1305	0.0596

param	[Cu <sub>2</sub> (L <sup>8</sup> ) <sub>2</sub> ·MeOH]	[Cu <sub>2</sub> (L <sup>5</sup> ) <sub>2</sub> ]	[Cu <sub>2</sub> (L <sup>6</sup> ) <sub>2</sub> ·2CHCl <sub>3</sub> ]	[Pd(L <sup>1</sup> )]
formula	C <sub>21</sub> H <sub>26</sub> Cu <sub>2</sub> N <sub>2</sub> O <sub>7</sub> S <sub>2</sub>	C <sub>18</sub> H <sub>18</sub> Cu <sub>2</sub> N <sub>2</sub> O <sub>6</sub>	C <sub>22</sub> H <sub>24</sub> Cl <sub>6</sub> Cu <sub>2</sub> N <sub>2</sub> O <sub>8</sub>	C <sub>16</sub> H <sub>14</sub> N <sub>2</sub> O <sub>2</sub> PdS <sub>2</sub>
cryst syst	monoclinic	monoclinic	monoclinic	monoclinic
space group	<i>C</i> 2/ <i>c</i>	<i>P</i> 2 <sub>1</sub> / <i>c</i>	<i>P</i> 2 <sub>1</sub> / <i>c</i>	<i>P</i> 2 <sub>1</sub> / <i>a</i>
<i>a</i> /Å	19.978(10)	5.1113(19)	8.757(3)	7.943(4)
<i>b</i> /Å	5.640(4)	17.603(9)	13.815(7)	19.877(8)
<i>c</i> /Å	22.144(10)	9.828(7)	12.839(5)	10.037(4)
$\alpha$ /deg				
$\beta$ /deg	115.35(2)	105.15(3)	108.501(17)	96.51(2)
$\gamma$ /deg				
<i>V</i> /Å <sup>3</sup>	2255(2)	853.5(8)	1473.0(11)	1574.4(12)
<i>Z</i>	4	2	2	4
<i>T</i> /K	120	120	120	120
<i>D</i> <sub>calc</sub> /g cm <sup>-3</sup>	1.796	1.889	1.768	1.843
R1 <sup>a</sup> [ <i>I</i> > 2 $\sigma$ ( <i>I</i> )]	0.0607	0.0407	0.0242	0.0391
wR2 <sup>a</sup> (all data)	0.1588	0.0887	0.0607	0.0895

$$^a \text{R1} = \sum ||F_o| - |F_c|| / \sum |F_c|; \text{wR2} = [\sum (w(F_o^2 - F_c^2)^2) / \sum (w(F_o^2)^2)]^{1/2}.$$

Scheme 1. Synthesis of the N<sub>2</sub>S<sub>2</sub> and N<sub>2</sub>SO Ligands<sup>a</sup>

<sup>a</sup> Reagents and conditions: (a) dichloromethane, rt, 47% (R = H, H<sub>2</sub>L<sup>1</sup>), 43% (R = OMe, H<sub>2</sub>L<sup>2</sup>); (b) ethanol, 50–55 °C, 81% (R = H; **5**),<sup>6b</sup> 71% (R = OMe; **6**);<sup>6b</sup> (c) dichloromethane, rt, 48% (R = H, H<sub>2</sub>L<sup>3</sup>), 55% (R = OMe, H<sub>2</sub>L<sup>4</sup>).

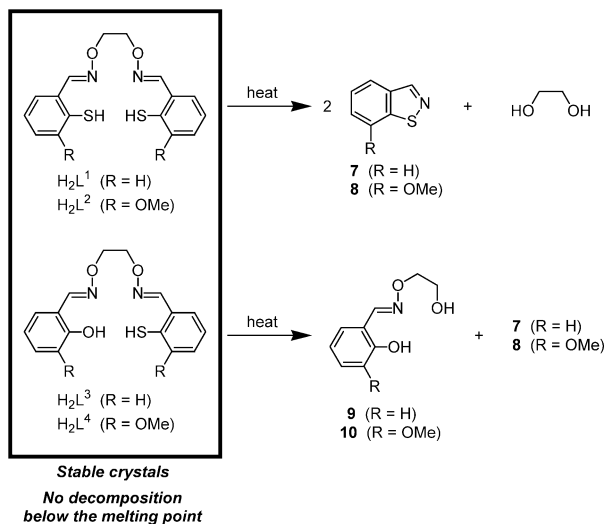
such N<sub>2</sub>SO ligands would be much more difficult for the following two reasons. One is the high reactivity of the thiosalicylaldehyde moiety as already described. The other is the C=N bond recombination of two different salicylaldehyde moieties leading to a statistical mixture.<sup>6</sup> Indeed, there has been only one report of a metal complex having a salen-type N<sub>2</sub>SO ligand,<sup>28</sup> which was prepared via bis-(thiosalicylaldehyde)nickel(II) as a synthetic intermediate.

The oxime functionality is expected to have sufficient stability to resist the undesired reactions, such as nucleophilic attack of thiols and recombination of C=N bonds.

The synthesis of the unsymmetrical N<sub>2</sub>SO ligands, i.e., H<sub>2</sub>L<sup>3</sup> and H<sub>2</sub>L<sup>4</sup>, is shown in Scheme 1. The *O*-(2-(aminooxy)-ethyl)oximes **5** and **6** were prepared according to the reported procedures<sup>6b</sup> from salicylaldehydes **3** and **4**, and the reaction of **5** and **6** with the corresponding thiosalicylaldehydes **1** and **2** afforded the N<sub>2</sub>SO ligands, H<sub>2</sub>L<sup>3</sup> and H<sub>2</sub>L<sup>4</sup>, as stable colorless crystals in 48% and 55% yield, respectively.

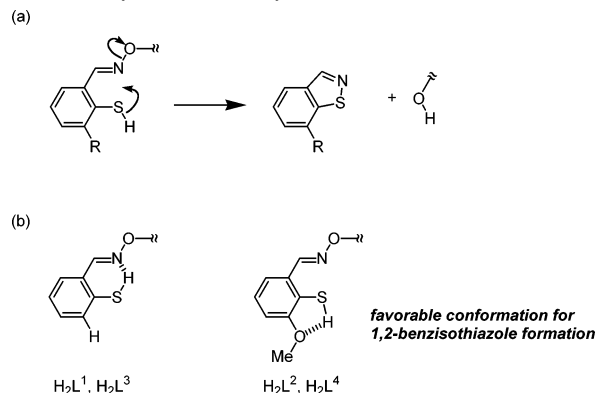
**Stability of the N<sub>2</sub>S<sub>2</sub> and N<sub>2</sub>SO Ligands.** As described above, the salen-type N<sub>2</sub>S<sub>2</sub> ligands (H<sub>2</sub>L<sup>1</sup> and H<sub>2</sub>L<sup>2</sup>) and N<sub>2</sub>-SO ligands (H<sub>2</sub>L<sup>3</sup> and H<sub>2</sub>L<sup>4</sup>) based on the oxime C=N bonds are synthesized as isolable crystals with melting points in the range from 50 to 90 °C. In order to investigate the thermal stability and limitation, ligands H<sub>2</sub>L<sup>1</sup>–H<sub>2</sub>L<sup>4</sup> were heated at 150 °C under an argon atmosphere. The parent H<sub>2</sub>salamo (H<sub>2</sub>L<sup>1</sup>) decomposed to give a mixture containing **7**<sup>23</sup> and ethylene glycol upon heating (Scheme 2). Thermal decomposition of the methoxy analogue, H<sub>2</sub>L<sup>2</sup>, afforded **8**.<sup>22</sup> A similar thermal decomposition of the N<sub>2</sub>SO ligands (H<sub>2</sub>L<sup>3</sup> and H<sub>2</sub>L<sup>4</sup>) afforded a mixture containing salicylaldehyde *O*-(2-hydroxyethyl)oximes (**9** and **10**) and 1,2-benzisothiazole derivatives (**7** and **8**). There are several reports that benzaldoximes having sulfur functionality at the ortho position afford 1,2-benzisothiazoles by heating<sup>23b,29</sup> and that oxidation

(28) Gomes, L.; Pereira, E.; de Castro, B. *J. Chem. Soc., Dalton Trans.* **2000**, 1373–1379.

**Scheme 2.** Thermolysis of  $N_2S_2$  ( $H_2L^1$  and  $H_2L^2$ ) and  $N_2SO$  ( $H_2L^3$  and  $H_2L^4$ ) Ligands

of some metal complexes containing the  $[Ni(\text{tsalen})]$  moieties affords 1,2-benzisothiazolium.<sup>30</sup> The formation of 1,2-benzisothiazole derivatives **7** and **8** was presumably due to the intramolecular attack of the thiol group on the oxime nitrogen (Scheme 3a). The formation of the N–S bond results in the five-membered isothiazole ring, and simultaneously, the alkoxide anion and proton are eliminated.

Although the  $N_2S_2$  and  $N_2SO$  ligands decomposed at higher temperature, these ligands were remarkably stable in solution at room temperature compared to the imine analogue. The  $^1H$  NMR spectra of  $H_2L^1$  and  $H_2L^3$  without methoxy groups (5 mM solution in degassed  $CDCl_3$ ) did not change even after 1 month. The methoxy derivatives,  $H_2L^2$  and  $H_2L^4$ , were slightly less stable under the same conditions. After 1 week, considerable amounts of **8** (and **10** in the case of  $H_2L^4$ ) were observed in the  $^1H$  NMR spectra, but the decomposition was negligible within 1 day. Obviously, the introduction of methoxy groups lowered the stability. This difference in stability can be explained by the conformation of the thiol group in the ligands. In the  $^1H$  NMR spectra, the thiol groups of  $H_2L^1$  and  $H_2L^3$  without methoxy groups were observed at 4.61 and 4.53 ppm, respectively, which indicates the existence of an intramolecular S–H $\cdots$ N hydrogen bond between the thiol group and the oxime nitrogen (Scheme 3b). This hydrogen bond fixes the conformation in such a way that the thiol group is directed toward the oxime nitrogen. In the case of the methoxy derivatives,  $H_2L^2$  and  $H_2L^4$ , the corresponding thiol protons were observed at 4.95 and 4.90 ppm, respectively, which were about 0.35 ppm lower than those of  $H_2L^1$  and  $H_2L^3$ .

**Scheme 3.** (a) Plausible Mechanism for the Formation of 1,2-Benzisothiazole Derivatives **7** and **8** and (b) Possible Conformation of the Thiosalicylaldoxime Moiety of  $H_2L^1$ – $H_2L^4$ 

This downfield shift is probably due to the contribution of the S–H $\cdots$ O hydrogen bond between the thiol group and the methoxy oxygen, in addition to the S–H $\cdots$ N one (Scheme 3b). The S–H $\cdots$ O hydrogen bond makes the conformation of the thiol group favorable for intramolecular attack to the  $sp^2$  nitrogen of the oxime moiety. This may result in faster S–N bond formation accompanying the elimination of the alkoxy group on the  $sp^2$  nitrogen.

**Synthesis, Structures, and Magnetic Properties of Nickel(II) Complexes.** The reaction of  $H_2L^1$  or  $H_2L^2$  with nickel(II) acetate in dichloromethane/methanol afforded the corresponding nickel(II) complexes as dark-brown crystals in 67 and 65% yield, respectively. The elemental analysis is consistent with the formula of the mononuclear complexes  $[Ni(L^1)]$  and  $[Ni(L^2)]$ . The ESI-MS spectra also confirmed the mononuclear structure. Furthermore, the  $^1H$  NMR spectra of the nickel(II) complexes showed sharp signals, indicative of the exclusive formation of a symmetrical and diamagnetic complex. The electronic absorption spectra showed a d–d transition (620 nm ( $\epsilon = 260$ ) for  $[Ni(L^1)]$  and 618 nm ( $\epsilon = 320$ ) for  $[Ni(L^2)]$ ) and a charge-transfer band (382 nm ( $\epsilon = 6000$ ) for  $[Ni(L^1)]$  and 392 nm ( $\epsilon = 7400$ ) for  $[Ni(L^2)]$ ), which are characteristic of low-spin square-planar nickel(II) complexes with  $N_2S_2$  coordination spheres.<sup>28</sup>

An X-ray crystallographic analysis revealed the mononuclear structures of the nickel complexes  $[Ni(L^1)]$  and  $[Ni(L^2)]$  (Figure 1 and Table 2). In both complexes, the four atoms of the  $N_2S_2$  donor set (N1, N2, S1, and S2) and Ni1 lie essentially in a plane. The dihedral angle between the two coordination planes, N1–Ni1–S1 and N2–Ni1–S2, is less than  $8^\circ$ , indicating almost an ideal square-planar geometry. It is noteworthy that the coordination bonds of one thiosalicylidene moiety (Ni1–N1 and Ni1–S1) are considerably shorter than those of the other (Ni1–N2 and Ni1–S2). Such differences are seen in some nickel(II) complexes of the thiosalicylidenediamine  $N_2S_2$  ligands.<sup>31</sup> In addition, there is a considerable difference between the two N–Ni–S angles. The angles N1–Ni1–S1 (at the “shorter” side) are around  $94^\circ$ , which are larger than the angles of N2–Ni1–S2 (at the “longer” side; around  $88^\circ$ ).

(29) (a) Clarke, K.; Hughes, C. G.; Scrowston, R. M. *J. Chem. Soc., Perkin Trans. 1* **1973**, 356–359. (b) Meth-Cohn, O.; Tarnowski, B. *Synthesis* **1978**, 58–60. (c) Lawson, A. J. *J. Chem. Soc., Chem. Commun.* **1981**, 1238–1239. (d) Lawson, A. J. *Phosphorus Sulfur* **1982**, *12*, 357–367. (e) Rahman, L. K. A.; Scrowston, R. M. *J. Chem. Soc., Perkin Trans. 1* **1984**, 385–390.

(30) (a) Kersting, B. *Eur. J. Inorg. Chem.* **1999**, 2157–2166. (b) Brooker, S.; Caygill, G. B.; Croucher, P. D.; Davidson, T. C.; Clive, D. L. J.; Magnuson, S. R.; Cramer, S. P.; Ralston, C. Y. *J. Chem. Soc., Dalton Trans.* **2000**, 3113–3121. (c) Goswami, N.; Van Stipdonk, M. J.; Eichhorn, D. M. *Inorg. Chem. Commun.* **2003**, *6*, 86–89.

(31) Frydendahl, H.; Toftlund, H.; Becher, J.; Dutton, J. C.; Murray, K. S.; Taylor, L. F.; Anderson, O. P.; Tiekink, E. R. T. *Inorg. Chem.* **1995**, *34*, 4467–4476.

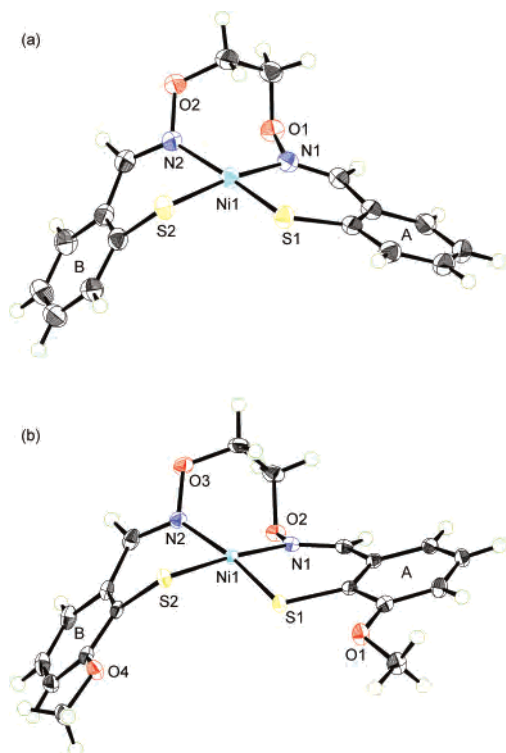


**Figure 1.** Crystal structures of (a)  $[\text{Ni}(\text{L}^1)]$  and (b)  $[\text{Ni}(\text{L}^2)]$  with thermal ellipsoids plotted at the 50% probability level.

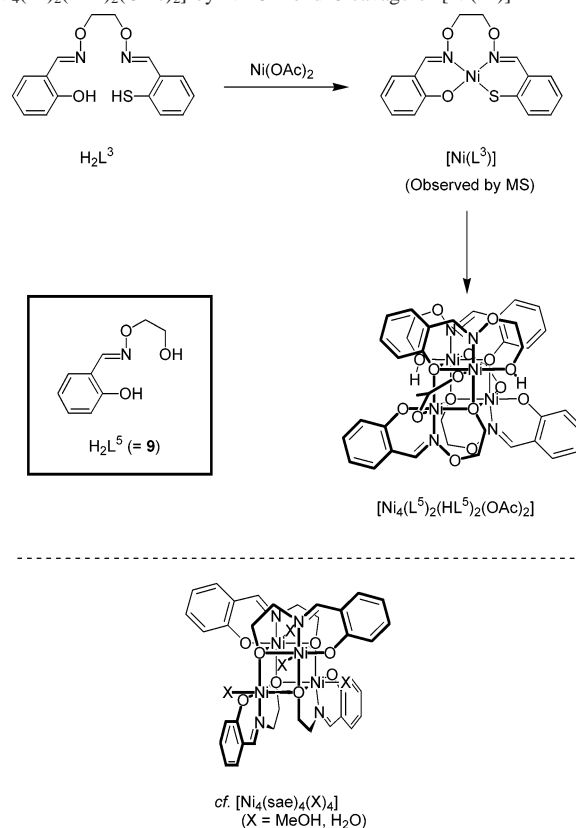
**Table 2.** Selected Geometrical Parameters of  $[\text{Ni}(\text{L}^1)]$  and  $[\text{Ni}(\text{L}^2)]$

	$[\text{Ni}(\text{L}^1)]$	$[\text{Ni}(\text{L}^2)]$
Distance (Å)		
Ni1–N1	1.897(2)	1.8761(16)
Ni1–N2	1.9462(19)	1.9446(15)
Ni1–S1	2.1399(6)	2.1533(8)
Ni1–S2	2.1973(7)	2.1848(9)
N1–S1	2.971(2)	2.9575(17)
N2–S2	2.871(2)	2.8932(16)
Bond Angle (deg)		
N1–Ni1–N2	95.02(8)	94.36(6)
S1–Ni1–S2	83.40(2)	82.52(2)
N1–Ni1–S1	94.57(6)	94.19(5)
N2–Ni1–S2	87.49(6)	88.76(4)
Dihedral Angle (deg)		
N1–Ni1–S1/N2–Ni1–S2	7.96(9)	4.44(6)
A/Ni1–N1–N2–S1–S2	14.6	24.4
B/Ni1–N1–N2–S1–S2	56.7	58.4

Although the geometries around the nickel atoms of  $[\text{Ni}(\text{L}^1)]$  and  $[\text{Ni}(\text{L}^2)]$  are quite similar, there is a difference in the conformations. Each of the two benzene rings of  $[\text{Ni}(\text{L}^1)]$  (A and B in Figure 1a) intersects downward from the Ni– $\text{N}_2\text{S}_2$  coordination plane, while one benzene ring of  $[\text{Ni}(\text{L}^2)]$  points upward (A in Figure 1b). In both complexes, the dihedral angle between the Ni– $\text{N}_2\text{S}_2$  plane and the benzene ring B ( $56$ – $59^\circ$ ) is considerably larger than that for the benzene ring A ( $14$ – $25^\circ$ ). The elongation of the coordination bonds (Ni1–S2 and Ni1–N2) indicates a weaker interaction of the ligand with the nickel center,<sup>31</sup> probably due to the distorted geometry of the complex.

In contrast to the complexation of the  $\text{N}_2\text{S}_2$  ligands with nickel(II) acetate, the reaction of the  $\text{N}_2\text{O}_2$  analogues,  $\text{H}_2$ -salamo and  $\text{H}_2$ (3-MeOsalamo), with nickel(II) acetate gave  $[\text{Ni}_3(\text{salamo})_2(\text{OAc})_2(\text{EtOH})_2]$  and  $[\text{Ni}(3\text{-MeOsalamo})(\text{H}_2\text{O})_2]$ , respectively.<sup>20</sup> All of the nickel atoms of the complex have

**Scheme 4.** Formation of the Tetranuclear Cluster  $[\text{Ni}_4(\text{L}^5)_2(\text{HL}^5)_2(\text{OAc})_2]$  by N–O Bond Cleavage of  $[\text{Ni}(\text{L}^3)]$



an octahedral geometry. The structural difference is probably related to the ligand field strength. The  $\text{N}_2\text{S}_2$  donor set of the tsalamo ligands ( $\text{H}_2\text{L}^1$  and  $\text{H}_2\text{L}^2$ ) provides a stronger ligand field, which stabilizes the low-spin square-planar complex.

In this context, the spin state of the nickel(II) complexes of the  $\text{N}_2\text{SO}$  ligand is of interest because the  $\text{N}_2\text{SO}$  site of  $\text{H}_2\text{L}^3$  and  $\text{H}_2\text{L}^4$  is expected to have an intermediate ligand field strength between the  $\text{N}_2\text{S}_2$  and  $\text{N}_2\text{O}_2$  ligands.<sup>28</sup> Thus, we investigated the synthesis of the mononuclear nickel(II) complex. When the  $\text{N}_2\text{SO}$  ligand  $\text{H}_2\text{L}^3$  was mixed with nickel(II) acetate, the color changed to brown. The sharp  $^1\text{H}$  NMR signals and mass peak at  $m/z = 373.0$  for  $[\text{Ni}(\text{L}^3) + \text{H}]^+$  indicate the formation of a low-spin square-planar complex  $[\text{Ni}(\text{L}^3)]$  (Scheme 4). From the solution, bluish-green single crystals were obtained instead of brown ones. The X-ray crystallographic analysis revealed the structure of the tetranuclear nickel(II) complex  $[\text{Ni}_4(\text{L}^5)_2(\text{HL}^5)_2(\text{OAc})_2]$ , having four molecules of **9** ( $=\text{H}_2\text{L}^5$ ) instead of the tetradentate  $\text{N}_2\text{SO}$  ligand  $\text{H}_2\text{L}^3$  (Figure 2 and Table 3). The complex has a  $\text{Ni}_4\text{O}_4$  cubane core consisting of four hexacoordinate nickel atoms and four  $\mu_3$ -oxygen donors. All of the four nickel atoms are in a distorted octahedral coordination sphere, consisting of five oxygen and one nitrogen donors. Two monodeprotonated ligands  $(\text{HL}^5)^-$  (O1–N1–O3 and O4–N2–O6) coordinate to the nickel centers (Ni1 and Ni2) in a *mer*-bischelating tridentate fashion, and the phenoxo oxygen donors (O1 and O4) make up the cubane core in a  $\mu_3$ -bridging fashion. The other two ligands (O7–N3–O9 and O10–N4–O12) are doubly deprotonated and act in a similar *mer*-bischelating tridentate fashion, but the  $\mu_3$ -alkoxo donors (O9



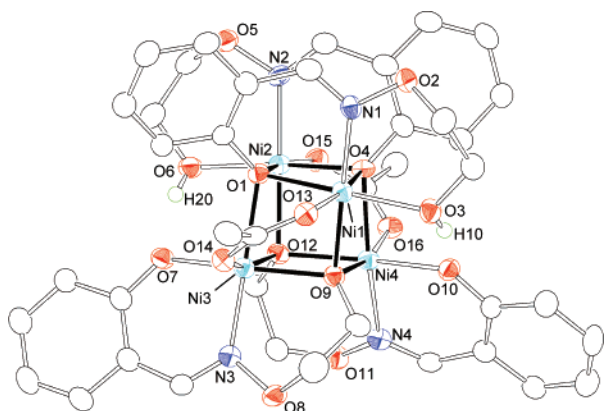


**Figure 2.** Crystal structure of the tetranuclear complex  $[\text{Ni}_4(\text{L}^5)_2(\text{HL}^5)_2(\text{OAc})_2]$  obtained by the reaction of the  $\text{N}_2\text{SO}$  ligand  $\text{H}_2\text{L}^3$  with nickel(II) acetate. Thermal ellipsoids are plotted at the 50% probability level. Hydrogen atoms except for OH groups (H10 and H20) and the minor component of disordered atoms are omitted for clarity.

**Table 3.** Selected Interatomic Distances and Angles of the Tetranuclear Nickel(II) Cluster  $[\text{Ni}_4(\text{L}^5)_2(\text{HL}^5)_2(\text{OAc})_2]$

Distance (Å)			
Ni1–Ni1	2.015(4)	Ni3–Ni3	2.025(4)
Ni1–O1	2.074(3)	Ni3–O1	2.157(3)
Ni1–O3	2.063(3)	Ni3–O7	2.011(3)
Ni1–O4	2.149(3)	Ni3–O9	2.039(3)
Ni1–O9	2.036(3)	Ni3–O12	2.097(3)
Ni1–O13	2.017(3)	Ni3–O14	2.034(3)
Ni2–Ni2	2.012(4)	Ni4–Ni4	2.038(4)
Ni2–O1	2.156(3)	Ni4–O4	2.138(3)
Ni2–O4	2.061(3)	Ni4–O9	2.101(3)
Ni2–O6	2.064(3)	Ni4–O10	2.004(3)
Ni2–O12	2.016(3)	Ni4–O12	2.037(3)
Ni2–O15	2.040(3)	Ni4–O16	2.032(3)
Ni1–Ni2	3.2659(12)	Ni2–Ni3	3.1275(11)
Ni1–Ni3	2.9489(10)	Ni2–Ni4	2.9474(10)
Ni1–Ni4	3.0996(11)	Ni3–Ni4	3.2452(11)
Angle (deg)			
O1–Ni1–O4	77.94(12)	Ni1–O1–Ni2	101.08(13)
O1–Ni1–O9	88.39(12)	Ni1–O1–Ni3	88.35(12)
O4–Ni1–O9	85.12(12)	Ni2–O1–Ni3	92.95(12)
O1–Ni2–O4	78.05(12)	Ni1–O4–Ni2	101.70(14)
O1–Ni2–O12	84.32(12)	Ni1–O4–Ni4	92.60(12)
O4–Ni2–O12	87.71(12)	Ni2–O4–Ni4	89.13(12)
O1–Ni3–O9	86.07(12)	Ni1–O9–Ni3	92.73(13)
O1–Ni3–O12	82.39(12)	Ni1–O9–Ni4	97.04(13)
O9–Ni3–O12	76.68(12)	Ni3–O9–Ni4	103.24(14)
O4–Ni4–O9	83.84(12)	Ni2–O12–Ni3	99.00(13)
O4–Ni4–O12	85.13(12)	Ni2–O12–Ni4	93.31(13)
O9–Ni4–O12	76.61(12)	Ni3–O12–Ni4	103.45(14)

and O12) form the cubane core instead of the phenoxo oxygen (O7 and O10). The hydroxyl groups (O3–H10 and O6–H20) of two monodeprotonated ligands  $(\text{HL}^5)^-$  participate in the intramolecular hydrogen bond to the alkoxo oxygen atoms (O10 and O7) of the bisdeprotonated ligands  $(\text{L}^5)^{2-}$  (O–H $\cdots$ O distances, 2.6–2.7 Å). In addition, two acetato ligands (O13–O14 and O15–O16) bridge the nickel atoms (Ni1–Ni3 and Ni2–Ni4) of the cubane core in a diagonal fashion.

An analogous imine-type ligand, 2-salicylideneaminoethanol ( $\text{H}_2\text{sae}$ ), forms tetranuclear clusters  $[\text{Ni}_4(\text{sae})_4\text{X}_4]$  ( $\text{X} = \text{MeOH}, \text{H}_2\text{O}$ ) bearing a similar  $\text{Ni}_4\text{O}_4$  cubane core (Scheme 4).<sup>32</sup> In these complexes, all four sae ligands are doubly deprotonated and their alkoxo oxygen atoms form the  $\text{Ni}_4\text{O}_4$  core, resulting in approximate  $S_4$  symmetry. Unlike these complexes,  $[\text{Ni}_4(\text{L}^5)_2(\text{HL}^5)_2(\text{OAc})_2]$  described here has a lower symmetry, because of the participation of  $\mu_3$ -phenoxo

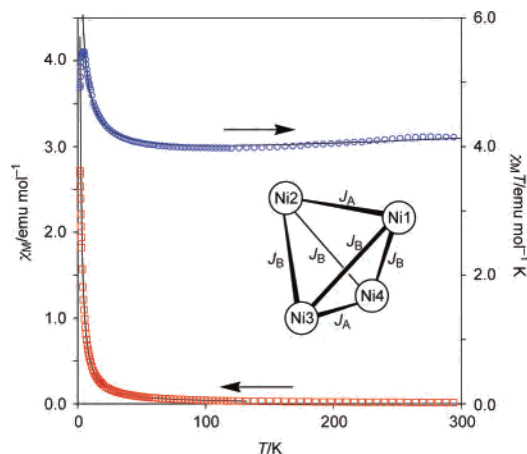


**Figure 3.** Plot of the  $\chi_M T$  product and  $\chi_M$  versus  $T$  for the tetranuclear complex  $[\text{Ni}_4(\text{L}^5)_2(\text{HL}^5)_2(\text{OAc})_2]$  measured in a 500 Oe field. Solid lines represent the best fit of the data described in the text.

groups and the coordination of  $\mu_2$ -acetato ligands. The O–Ni bonds O1–Ni2, O1–Ni3, O4–Ni1, and O4–Ni4, involving the phenoxo oxygen, are considerably elongated (2.138–2.157 Å). It is noteworthy that two of the six faces of the cubane framework considerably distort to give longer Ni $\cdots$ Ni separations [Ni1–Ni2, 3.2659(12) Å; Ni3–Ni4, 3.2452(11) Å] and larger Ni–O–Ni angles (101–104°).

There are a number of reports on the magnetochemistry of tetranuclear complexes having a  $\text{Ni}_4\text{O}_4$  cubane core. The intramolecular magnetic interactions are closely related to the Ni–O–Ni angles; they are ferromagnetic for angles close to orthogonality and antiferromagnetic for larger angles.<sup>33</sup> Accordingly, in the case of  $[\text{Ni}_4(\text{L}^5)_2(\text{HL}^5)_2(\text{OAc})_2]$ , the ferro- and antiferromagnetic interactions might be operative. Variable-temperature magnetic susceptibility measurement was performed on samples of  $[\text{Ni}_4(\text{L}^5)_2(\text{HL}^5)_2(\text{OAc})_2]$  at 500 Oe in the temperature range of 1.8–300 K (Figure 3). The  $\chi_M T$  value at 300 K (4.15 emu mol<sup>-1</sup> K) corresponds to the spin-only value for four noninteracting nickel(II) centers (4.0 emu mol<sup>-1</sup> K with  $g = 2$ ). As the temperature was lowered, the  $\chi_M T$  value gradually increased to a maximum value of 5.48 emu mol<sup>-1</sup> K at 5.0 K. This behavior suggests that the overall ferromagnetic intramolecular interactions are operative among the nickel(II) centers. The decrease of  $\chi_M T$  below 5 K can be attributed to zero-field splitting and/or intermolecular antiferromagnetic interactions. The data were analyzed by using the spin Hamiltonian (eq 1), where  $J_A$  characterizes the ex-

$$\hat{H} = -2J_A(\hat{S}_1 \cdot \hat{S}_2 + \hat{S}_3 \cdot \hat{S}_4) - 2J_B(\hat{S}_1 \cdot \hat{S}_3 + \hat{S}_1 \cdot \hat{S}_4 + \hat{S}_2 \cdot \hat{S}_3 + \hat{S}_2 \cdot \hat{S}_4) \quad (1)$$

change interaction across the two distorted faces (Ni1–Ni2 and Ni3–Ni4) with larger Ni–O–Ni angles, while  $J_B$  char-

(32) (a) Boskovic, C.; Rusanov, E.; Stoeckli-Evans, H.; Güdel, H. U. *Inorg. Chem. Commun.* **2002**, *5*, 881–886. (b) Nihei, M.; Hoshino, N.; Ito, T.; Oshio, H. *Polyhedron* **2003**, *22*, 2359–2362. (c) Sieber, A.; Boskovic, C.; Bircher, R.; Waldmann, O.; Ochsenbein, S. T.; Chaboussant, G.; Güdel, H. U.; Kirchner, N.; van Slageren, J.; Wernsdorfer, W.; Neels, A.; Stoeckli-Evans, H.; Janssen, S.; Juranyi, F.; Mutka, H. *Inorg. Chem.* **2005**, *44*, 4315–4325.

(33) Clemente-Juan, J. M.; Chansou, B.; Donnadieu, B.; Tuchagues, J.-P. *Inorg. Chem.* **2000**, *39*, 5515–5519.



acterizes the remaining four pairwise interactions (Figure 3). The least-squares calculation yielded the best-fit parameters of the  $J_A$  and  $J_B$  values of  $-0.45(5)$  and  $+1.02(4)$   $\text{cm}^{-1}$ , respectively, with  $g = 1.95$ .<sup>34</sup> The negative  $J_A$  and positive  $J_B$  are in good agreement with the structural feature described above.

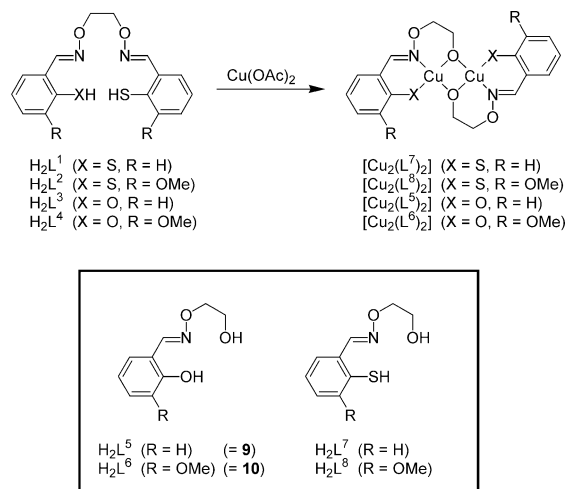
In the formation process of the tetranuclear cluster  $[\text{Ni}_4(\text{L}^5)_2(\text{HL}^5)_2(\text{OAc})_2]$ , the oxime N–O bond of the  $N_2SO$  ligand  $\text{H}_2\text{L}^3$  was cleaved. As described above, the mononuclear complex  $[\text{Ni}(\text{L}^3)]$  was initially formed in the reaction mixture of the  $N_2SO$  ligand  $\text{H}_2\text{L}^3$  with nickel(II) acetate. The gradual transformation of  $[\text{Ni}(\text{L}^3)]$  to tetranuclear  $[\text{Ni}_4(\text{L}^5)_2(\text{HL}^5)_2(\text{OAc})_2]$  probably took place during the recrystallization process (Scheme 4). In this process, the N–O bond in the thiosalicylaldehyde moiety was cleaved, and the 1,2-benzisothiazole ring or nitrile functionality was possibly formed.<sup>35</sup> Obviously, complexation with nickel(II) accelerated the N–O bond cleavage of ligand  $\text{H}_2\text{L}^3$  because the uncomplexed ligand  $\text{H}_2\text{L}^3$  did not change in solution after 1 month.

**Complexation with Copper(II).** The synthesis of copper(II) complexes of the  $N_2S_2$  and  $N_2SO$  ligands  $\text{H}_2\text{L}^1$ – $\text{H}_2\text{L}^4$  was investigated in a similar manner. There are some examples of mononuclear copper(II) complexes of salen ligands, whose structures were determined by X-ray crystallography.<sup>14b</sup> When an  $N_2S_2$  ligand,  $\text{H}_2\text{L}^1$  or  $\text{H}_2\text{L}^2$ , was mixed with copper(II) acetate in dichloromethane/methanol, yellowish-brown precipitates immediately formed. Recrystallization of the products gave dark-brown needles suitable for X-ray crystallography. Contrary to the expectation, these are dinuclear complexes  $[\text{Cu}_2(\text{L}^7)_2]$  and  $[\text{Cu}_2(\text{L}^8)_2]$ , having two thiosalicylaldehyde *O*-(2-hydroxyethyl)oxime ligands ( $\text{H}_2\text{L}^7$  for  $\text{R} = \text{H}$  and  $\text{H}_2\text{L}^8$  for  $\text{R} = \text{OMe}$ ) instead of the  $N_2S_2$  ligands (Scheme 5). The reaction of the  $N_2SO$  ligands  $\text{H}_2\text{L}^3$  and  $\text{H}_2\text{L}^4$  with copper(II) acetate afforded similar dinuclear complexes  $[\text{Cu}_2(\text{L}^5)_2]$  and  $[\text{Cu}_2(\text{L}^6)_2]$ , respectively, which have phenoxo oxygen atoms instead of sulfur.

These four complexes ( $[\text{Cu}_2(\text{L}^7)_2]$ ,  $[\text{Cu}_2(\text{L}^8)_2]$ ,  $[\text{Cu}_2(\text{L}^5)_2]$ , and  $[\text{Cu}_2(\text{L}^6)_2]$ ) have similar centrosymmetric dinuclear structures (Figure 4 and Table 4). In the case of sulfur complexes, an S–N–O tridentate ligand,  $(\text{L}^7)^{2-}$  or  $(\text{L}^8)^{2-}$ , coordinates to the copper atom in a *mer*-bischelating fashion. In the case of phenoxo complexes, the ligand  $(\text{L}^5)^{2-}$  or  $(\text{L}^6)^{2-}$  coordinates to the copper atoms in an O–N–O fashion. An additional  $\mu_2$ -alkoxo group (O2\* for  $[\text{Cu}_2(\text{L}^7)_2]$ , O3\* for  $[\text{Cu}_2(\text{L}^8)_2]$  and  $[\text{Cu}_2(\text{L}^5)_2]$ , and O4\* for  $[\text{Cu}_2(\text{L}^6)_2]$  in Figure 4) completes the square-planar geometry.

These dinuclear complexes have a planar four-membered  $\text{Cu}_2\text{O}_2$  core, distorted in such a way that makes a longer  $\text{Cu}\cdots\text{Cu}$  separation. The Cu–O–Cu and O–Cu–O angles are  $103.4$ – $104.7^\circ$  and  $75.3$ – $76.6^\circ$ , respectively. The Cu–alkoxo and Cu–N distances in the thiolato complexes  $[\text{Cu}_2(\text{L}^7)_2]$  and  $[\text{Cu}_2(\text{L}^8)_2]$  (Cu–O,  $1.933$ – $1.946$  Å; Cu–N,  $1.953$ – $1.959$  Å) are longer than those in the corresponding phenoxo complexes  $[\text{Cu}_2(\text{L}^5)_2]$  and  $[\text{Cu}_2(\text{L}^6)_2]$  (Cu–O,

**Scheme 5.** Complexation of  $N_2S_2$  and  $N_2SO$  Ligands with Copper(II) Acetate



$1.906$ – $1.922$  Å; Cu–N,  $1.928$ – $1.938$  Å). The N–Cu–S angles ( $96.2^\circ$ ) in the thiolato complexes  $[\text{Cu}_2(\text{L}^7)_2]$  and  $[\text{Cu}_2(\text{L}^8)_2]$  are larger than the N–Cu–O angles in the corresponding oxygen analogues  $[\text{Cu}_2(\text{L}^5)_2]$  and  $[\text{Cu}_2(\text{L}^6)_2]$  ( $93.0$ – $93.8^\circ$ ), because of the longer Cu–S bonds ( $2.22$ – $2.24$  Å) in  $(\text{L}^7)^{2-}$  and  $(\text{L}^8)^{2-}$ .

Although the sulfur-containing complexes  $[\text{Cu}_2(\text{L}^7)_2]$  and  $[\text{Cu}_2(\text{L}^8)_2]$  were obtained in very low yield (less than 10%), the isolated yields of the oxygen analogues  $[\text{Cu}_2(\text{L}^5)_2]$  and  $[\text{Cu}_2(\text{L}^6)_2]$  are rather high (52%). The N–O bond in the thiosalicylaldehyde moiety is probably more readily cleaved than that in the salicylaldehyde moiety. As a result, the thiosalicylideneamino group is selectively eliminated from the  $N_2SO$  ligands  $\text{H}_2\text{L}^3$  and  $\text{H}_2\text{L}^4$  to give the O–N–O tridentate ligands  $(\text{L}^5)^{2-}$  and  $(\text{L}^6)^{2-}$ , which are capable of forming dinuclear copper(II) complexes.

Analogous dinuclear copper(II) complexes have been prepared from 2-(salicylideneamino)ethanol and 3-(salicylideneamino)propanol derivatives, which have an imine group instead of the oxime of  $\text{H}_2\text{L}^5$  or  $\text{H}_2\text{L}^6$ .<sup>36</sup> The geometrical feature of the alkoxo-bridged Cu–O–Cu–O core is similar to that of  $[\text{Cu}_2(\text{L}^5)_2]$  and  $[\text{Cu}_2(\text{L}^6)_2]$ . Alkoxo groups are more likely to bridge two copper(II) ions than phenoxo groups. On the other hand, there have been no reports on the imine analogue of the sulfur-containing dinuclear complexes  $[\text{Cu}_2(\text{L}^7)_2]$  and  $[\text{Cu}_2(\text{L}^8)_2]$ . In the present study, we have demonstrated that S–N–O tridentate ligands based on oxime/thiol groups can also form alkoxo-bridged dinuclear copper(II) complexes having a four-membered Cu–O–Cu–O core.

We investigated the magnetic properties originating from the  $\text{Cu}_2\text{O}_2$  core. The magnetic susceptibility of  $[\text{Cu}_2(\text{L}^5)_2]$  was measured at 500 Oe in the temperature range of  $1.8$ – $300$  K. The observed  $\chi_{\text{MT}}$  value at 300 K was  $0.119$   $\text{emu mol}^{-1}$  K, which is considerably lower than the spin-only

(34) The relatively smaller  $g$  value is presumably due to contamination of the diamagnetic impurity.

(35) Fierro, C. M.; Murphy, B. P.; Smith, P. D.; Coles, S. J.; Hursthouse, M. B. *Inorg. Chim. Acta* **2006**, *359*, 2321–2327.

(36) For examples, see: (a) Kato, M.; Muto, Y.; Jonassen, H. B.; Imai, K.; Harano, A. *Bull. Chem. Soc. Jpn.* **1968**, *41*, 1864–1870. (b) Miners, J. O.; Sinn, E. *Bull. Chem. Soc. Jpn.* **1973**, *46*, 1457–1461. (c) Nassiff, P. J.; Boyko, E. R.; Thompson, L. D. *Bull. Chem. Soc. Jpn.* **1974**, *47*, 2321–2322.

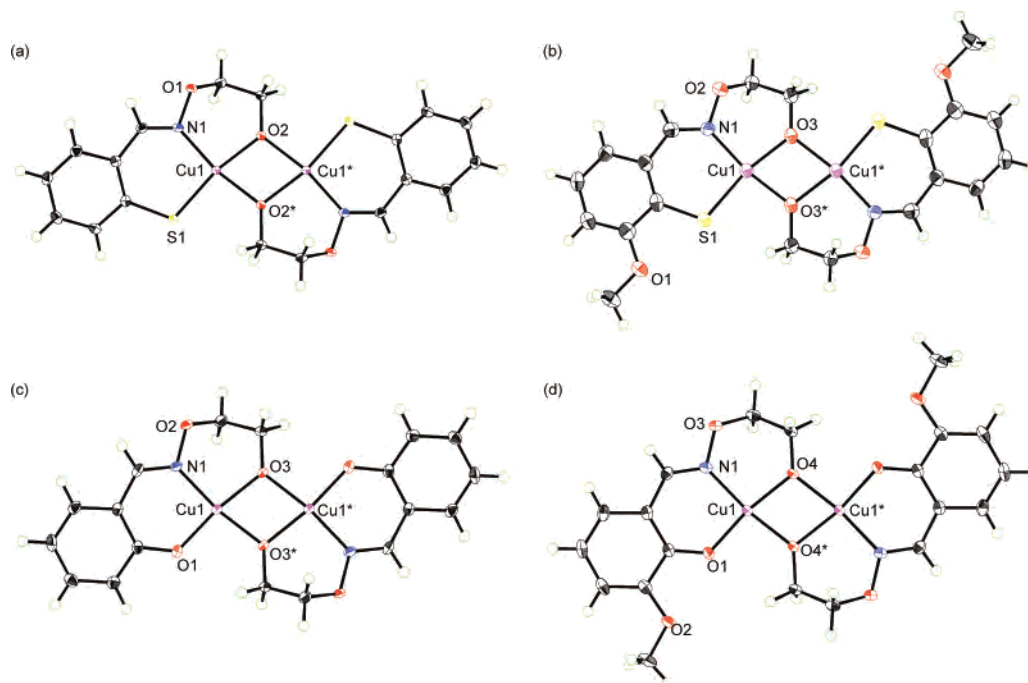


**Figure 4.** Crystal structure of dinuclear complexes (a)  $[\text{Cu}_2(\text{L}^7)_2]$ , (b)  $[\text{Cu}_2(\text{L}^8)_2]$ , (c)  $[\text{Cu}_2(\text{L}^5)_2]$ , and (d)  $[\text{Cu}_2(\text{L}^6)_2]$ . Thermal ellipsoids are plotted at the 50% probability level.

**Table 4.** Geometrical Parameters of Copper(II) Complexes  $[\text{Cu}_2(\text{L}^7)_2]$ ,  $[\text{Cu}_2(\text{L}^8)_2]$ ,  $[\text{Cu}_2(\text{L}^5)_2]$ , and  $[\text{Cu}_2(\text{L}^6)_2]$ <sup>a</sup>

	$[\text{Cu}_2(\text{L}^7)_2]$	$[\text{Cu}_2(\text{L}^8)_2]$	$[\text{Cu}_2(\text{L}^5)_2]$	$[\text{Cu}_2(\text{L}^6)_2]$			
	Distance (Å)						
Cu1–S1	2.2365(14)	Cu1–S1	2.2244(18)	Cu1–O1	1.891(3)	Cu1–O1	1.8847(12)
Cu1–N1	1.9591(19)	Cu1–N1	1.953(5)	Cu1–N1	1.928(3)	Cu1–N1	1.9384(14)
Cu1–O2	1.9455(18)	Cu1–O3	1.934(4)	Cu1–O3	1.909(2)	Cu1–O4	1.9056(12)
Cu1–O2 <sup>#1</sup>	1.9326(16)	Cu1–O3 <sup>#2</sup>	1.936(4)	Cu1–O3 <sup>#3</sup>	1.922(3)	Cu1–O4 <sup>#4</sup>	1.9190(12)
Cu1–Cu1 <sup>#1</sup>	3.0713(19)	Cu1–Cu1 <sup>#2</sup>	3.0616(19)	Cu1–Cu1 <sup>#3</sup>	3.0074(14)	Cu1–Cu1 <sup>#4</sup>	3.0090(10)
	Angle (deg)						
S1–Cu1–N1	96.21(6)	S1–Cu1–N1	96.16(14)	O1–Cu1–N1	93.00(12)	O1–Cu1–N1	93.82(6)
N1–Cu1–O2	94.53(7)	N1–Cu1–O3	95.12(18)	N1–Cu1–O3	94.82(12)	N1–Cu1–O4	95.44(6)
O2–Cu1–O2 <sup>#1</sup>	75.26(8)	O3–Cu1–O3 <sup>#2</sup>	75.42(19)	O3–Cu1–O3 <sup>#3</sup>	76.55(12)	O4–Cu1–O4 <sup>#4</sup>	76.24(6)
O2 <sup>#1</sup> –Cu1–S1	93.54(6)	O3 <sup>#2</sup> –Cu1–S1	92.86(13)	O3 <sup>#3</sup> –Cu1–O1	95.56(12)	O4 <sup>#4</sup> –Cu1–O1	94.78(5)
Cu1–O2–Cu1 <sup>#1</sup>	104.74(8)	Cu1–O3–Cu1 <sup>#2</sup>	104.58(19)	Cu1–O3–Cu1 <sup>#3</sup>	103.45(12)	Cu1–O4–Cu1 <sup>#4</sup>	103.76(6)

<sup>a</sup> Symmetry transformation used to generate equivalent atoms: #1,  $-x, -y + 1, -z + 2$ ; #2,  $-x + 1/2, -y + 3/2, -z$ ; #3,  $-x + 1, -y + 1, -z + 1$ ; #4,  $-x, -y, -z$ .

value expected for two noninteracting copper(II) centers ( $0.750 \text{ emu mol}^{-1} \text{ K}$  with  $g = 2.0$ ). Upon lowering of the temperature, the  $\chi_{\text{M}}T$  value decreases steadily to  $0.0021 \text{ emu mol}^{-1} \text{ K}$  at 1.8 K (Figure 5). This behavior clearly indicates that the antiferromagnetic interaction is dominant in the dinuclear system. The exchange coupling constant  $J$  was roughly estimated to be  $-500 \text{ cm}^{-1}$  using the spin Hamiltonian  $\hat{H} = -2J\hat{S}_1\cdot\hat{S}_2$ . It is reported that the exchange coupling constant  $J$  of such  $\text{Cu}_2\text{O}_2$  dinuclear complexes closely correlates with the Cu–O–Cu angle.<sup>37</sup> The large Cu–O–Cu angle ( $103.45^\circ$ ) is responsible for the strong antiferromagnetic interactions in  $[\text{Cu}_2(\text{L}^5)_2]$ .

**Synthesis of Palladium(II) Complexes.** The reaction of the  $\text{N}_2\text{S}_2$  ligand  $\text{H}_2\text{L}^1$  with palladium(II) acetate afforded reddish-orange crystals of the mononuclear palladium(II) complex  $[\text{Pd}(\text{L}^1)]$ , which was characterized by its elemental analysis and  $^1\text{H}$  NMR and MS spectra (Scheme 6). The X-ray

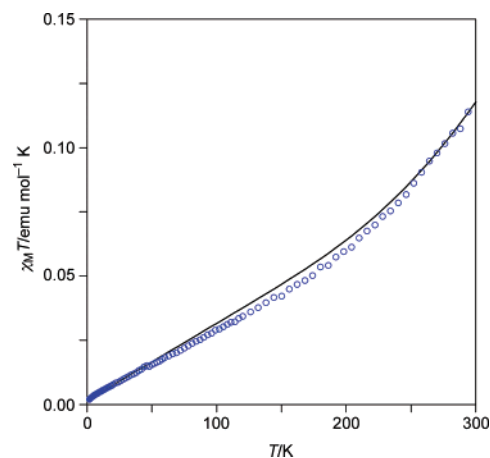


**Figure 5.** Plot of  $\chi_{\text{M}}T$  versus  $T$  measured in a 500 Oe field for the dinuclear complex  $[\text{Cu}_2(\text{L}^5)_2]$ . The solid line represents the fitted curve based on  $J = -500 \text{ cm}^{-1}$ .

crystallographic analysis revealed the structure of the complex  $[\text{Pd}(\text{L}^1)]$  (Figure 6), which is isostructural with the

(37) Lewis, D. L.; Hatfield, W. E.; Hodgson, D. J. *Inorg. Chem.* **1972**, *11*, 2216–2221.

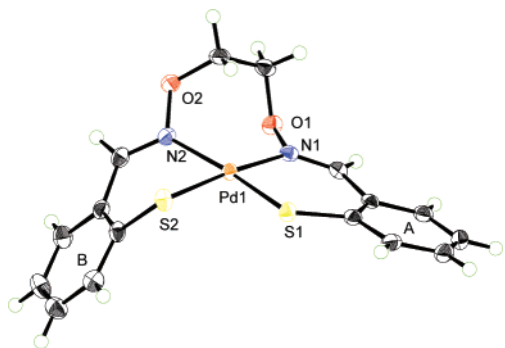
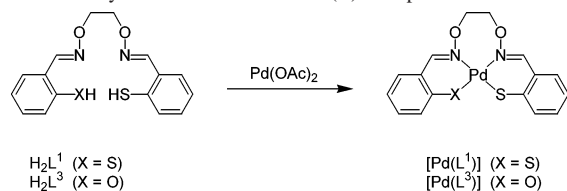


**Figure 6.** Crystal structure of  $[Pd(L^1)]$  with thermal ellipsoids plotted at the 50% probability level.

**Scheme 6.** Synthesis of the Palladium(II) Complex



nickel(II) analogue  $[Ni(L^1)]$ . The square-planar geometry around the palladium atom is obvious because the angle between the two coordination planes  $N1-Pd1-S1$  and  $N2-Pd1-S2$  is  $4.5^\circ$ . As in the case of  $[Ni(L^1)]$ , the bond lengths in one thiosalicylidene moiety [ $Pd1-N1$ , 2.036(3) Å;  $Pd1-S1$ , 2.2418(11) Å] are considerably shorter than those of the other [ $Pd1-N2$ , 2.092(3) Å;  $Pd1-S2$ , 2.2855(12) Å]. The dissymmetric feature is presumably attributed to the conformational distortion.

In a similar manner, the reaction of the  $N_2SO$  ligand  $H_2L^3$  with palladium(II) acetate was carried out and produced a reddish-orange powder of the complex. The  $^1H$  NMR and MS spectra as well as the elemental analysis are consistent with the mononuclear complex  $[Pd(L^3)]$ . In this case, ligand  $H_2L^3$  formed a mononuclear complex, in which  $(L^3)^{2-}$  acts as a tetradentate ligand with an  $N_2SO$  donor set, without cleavage of the  $N-O$  bond.

## Conclusion

We have synthesized the new salen-type  $N_2S_2$  tetradentate ligands,  $H_2L^1$  and  $H_2L^2$ , which have a donor set comprising

oxime and thiol groups. These ligands are obtained as isolable colorless crystals, whereas the imine analogues are too unstable to be isolated. The unsymmetrical  $N_2SO$  ligands,  $H_2L^3$  and  $H_2L^4$ , were also obtained as stable compounds. When ligands  $H_2L^1-H_2L^4$  were heated above the melting points, they mainly decomposed via cleavage of the  $N-O$  bonds of a thiosalicylaldehyde moiety to give 1,2-benzisothiazole derivatives. The complexation of the  $N_2S_2$  ligands ( $H_2L^1$  and  $H_2L^2$ ) with nickel(II) acetate afforded square-planar mononuclear complexes  $[Ni(L^1)]$  and  $[Ni(L^2)]$ , respectively. In contrast, the complexation of the  $N_2SO$  ligand  $H_2L^3$  with nickel(II) acetate resulted in cleavage of the  $N-O$  bond, giving a tetranuclear complex having a cubane-type  $Ni_4O_4$  core. The  $N-O$  bonds of  $H_2L^1-H_2L^4$  are more readily cleaved when the ligands are allowed to react with copper(II) acetate. In these cases, the alkoxy-bridged dinuclear complexes having a  $Cu-O-Cu-O$  four-membered ring are obtained. On the other hand, mononuclear complexes can be obtained by complexation of the ligands ( $H_2L^1$  or  $H_2L^3$ ) with palladium(II) acetate without  $N-O$  bond cleavage. Thus, we developed a new series of thiol-containing ligands called "tsalamo", which are much more stable than the imine analogues. The tsalamo and its analogues may be promising units for the construction of more complicated metalloarchitectures that have sulfur-containing chelate moieties, such as an  $N_2S_2$  or  $N_2SO$  coordination environment.

**Acknowledgment.** This work was supported by Grants-in-Aid for Scientific Research from the Ministry of Education, Culture, Sports, Science, and Technology, Japan.

**Note Added after ASAP Publication.** This article was released ASAP on January 9, 2008 with minor errors in Table 2. The correct version was posted on January 10, 2008.

**Supporting Information Available:** X-ray crystallographic data in CIF format. This material is available free of charge via the Internet at <http://pubs.acs.org>.

IC701525C